X CONGRESSO NACIONAL DE ENGENHARIA MECÂNICA 2018
20 A 24 DE MAIO DE 2018 SALVADOR – BA – BRASIL

# NUMERICAL AND EXPERIMENTAL ANALYSIS OF A NON-IDEAL TYPE SYSTEM

**Adriano Kossoski, adrianoutf@gmail.com**[1]
**Angelo Marcelo Tusset, a.m.tusset@gmail.com**[1]
**Gerson Henrique dos Santos, gsantos@utfpr.edu.br**[1]
**Rodrigo Tumolim Rocha, digao.rocha@gmail.com**[1]
**Frederic Conrad Janzen, fcjanzen@utfpr.edu.br**[1]
**Wagner Barth Lenz, wagner_barth@hotmail.com**[1]
**José Manoel Balthazar, jmbaltha@gmail.com**[1]

[1]UTFPR - Federal University of Technology - Paraná, 84016-210, Ponta Grossa - PR, Brazil

***Abstract:*** *Mechanical vibrations are an important research area due to the impact that this phenomenon can have on any system or machine. One class of vibration-related problems that are gaining ground in current research are the non-ideal or finite-energy systems. In a non-ideal type system, at the same time that the excitation source destabilizes the system, it is influenced by its own performance, losing energy. In this type of system, when the angular frequency of the excitation source approaches numerically a value similar to the natural frequency of the structure, the increase of energy in the system stops to relate to the increase of rotation or work of the energy source and ends up serving only to increase the vibration amplitudes of the system. This work aims to present both analytical and experimental analysis of a non-ideal system. The built system consists of a cantilever beam with an unbalanced DC motor at its tip. In the analytical part, the system had its equations obtained and later simulated numerically with the aid of Matlab® software. An equivalent system was constructed experimentally and, with the aid of a data acquisition system, experimental results for the non-ideal behavior of the system were obtained. The analytical results were compared with the experimental results, where it is possible to observe the similarity and thus the functionality of the mathematical model.*

***Keywords:*** *Non-ideal, Vibration, Sommerfeld Effect, Limited Power Supply, Jump Phenomena*

## 1. INTRODUCTION

In current engineering, systems that are composed of mechanical structures and rotary systems (motors, shafts, etc.) are extremely common configurations to be found in the most diverse designs and areas. These systems, like all dynamic systems, are susceptible to several types of mechanical vibrations. The mechanical vibration can cause malfunctions, shortened life cycles and catastrophic failures in machines and devices thus, should always be avoided or controlled in engineering projects. This makes this area of great importance in the project and design of a new machines, making it also important to know and understand the behavior that the system will present when in operation. Over time, various classifications and types of vibrations have been defined and among all these vibratory systems, stand out the systems classified as non-ideal (Balthazar *et al.*, 2003; Castão *et al.*, 2008 and Felix *et al.*, 2005).

Non-ideal systems are characterized by an energy exchange between the power source and the mechanical structure. In this kind of system, the power source, which commonly is an electric motor or another kind of rotating device, loses part of its energy which is converted in mechanical vibrations. This occurs when the value of the angular frequency of the power source approaches a value similar to some natural frequency of the system. in other words, the system demonstrates normal operation, but when the rotation of the unbalanced power source approaches the resonance region, the addition of energy at the source stops to correspond to an increase of rotation (work), that energy begins to only increase the amplitudes of vibration. When the system is able to pass through the resonance region, the vibration amplitudes drop abruptly, this is one of the reasons for this effect to be known as jump effect, jump phenomena or Sommerfeld Effect (Kononenko, 1969; Balthazar *et al.*, 2003 and Kossoski *et al.*, 2018).

Any dynamical system with some type of rotating device may exhibit the non ideal behavior, where systems with motors and engines are the most common. In practice, the Sommerfeld Effect can be seen easily in systems with large unbalance, where the system is destabilized at low operating frequencies.

In the mathematical modeling of dynamical systems, the system can be an ideal system, where the influence of the

power supply on the behavior of the structure is not considered or the system can be classified as non-ideal, where consideration must be given to the influence of the energy source on the behavior of the mechanical system. When a system is considered to be of the non-ideal type, the equations of the energy source (e.g., AC/DC motors, engines, etc) must be coupled with the mechanical equations. Due to the coupling between the mechanical system and the power supply system, the equations of this kind of system are more complex than when considering and ideal system (Balthazar *et al.*, 2003).

Thus, the purpose of this paper is to show a numerical and experimental investigation of a system classified as non-ideal. The system in question is composed of a cantilever aluminum beam and an unbalanced DC motor coupled at its free end. For the numerical analysis, the constitutive equations are obtained and simulated numerically. An equivalent system is then constructed and through a data acquisition system the Sommerfeld Effect is analyzed in the system, where the results of the simulation are compared with the experimental results.

## 2. MATHEMATICAL MODEL AND NUMERICAL SIMULATIONS

### 2.1 Mathematical Model

A non-ideal system consisting of a cantilever beam and an unbalanced DC motor at its free end is considered. For the mathematical model, the consideration of a lumped-parameter system was made. This system is shown in Fig. 1.

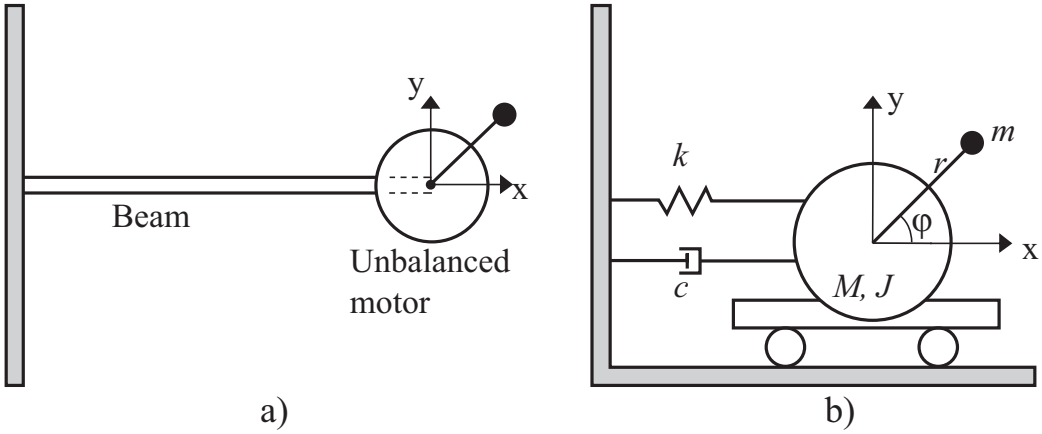


Figure 1: **Non-ideal system. a) Real system; b) Equivalent numerical system (Adapted from Balthazar *et al.*, 2003).**

Figure 1a shows a schematic of the real system and the Fig. 1b features the mass-spring-damper system considered for the model, where $k$ is the stiffness, $c$ is the damping, $M$ is the total mass of the beam with the motor, $J$ is the inertia of internal parts of the motor, $m$ is the unbalanced mass and $\varphi$ is the angle of the motor shaft. In this work, the Lagrangian Equations are used to obtain the mathematical model of the dynamic system. In this method, equations of the system motion can be written in the form of Eq. (1).

$$\frac{d}{dt}\left(\frac{\partial L_g}{\partial \dot{q}_i}\right) - \left(\frac{\partial L_g}{\partial q_i}\right) = 0 \tag{1}$$

Where $L_g$ is the Lagrange function and $q_i$ is a set of generalized coordinates. The Lagrange function depends of two energies, the kinetic energy and the potential energy. The kinetic energy ($E_k$) of the system is given by Eq. (2).

$$E_k = \frac{1}{2}M\dot{x}^2 + \frac{1}{2}J\varphi^2 + \frac{m}{2}\left(\dot{X}^2 + \dot{Y}^2\right) \tag{2}$$

Where $X = x + rsin(\varphi)$ and $Y = r(1 - cos(\varphi))$ are the functions that define the location of the unbalanced mass in the Cartesian plane.

The potential energy ($E_p$) is given by the Eq. (3).

$$E_p = \frac{1}{2}kx^2 \tag{3}$$

Substituting the Eq. (2) and Eq. (3) in the Eq. (1), one gets the representative equations of the non-ideal system in study, shown in Eq. (4) and Eq. (5).

$$M\ddot{x} + c\dot{x} + kx - mr(\dot{\varphi}^2 sin\varphi + \ddot{\varphi}cos\varphi) = 0 \tag{4}$$

$$\left(J + mr^2\right)\ddot{\varphi} + mr\ddot{x}cos\varphi = S(\dot{\varphi}) \tag{5}$$

Where $S(\dot{\varphi})$ is a resultant torque function generated by the motor. As the objective of this work is to obtain a complete model, both in the dynamic part as in the electric part, we look for the equations that represent an DC (Direct Current) electric motor.

Figure 2 shows a schematic of a permanent magnet type DC motor, where $R$ is the armature resistance, $L$ is the armature inductance, $i$ is the electric current through the motor and $T$ is the torque generated (Nise, 2007).

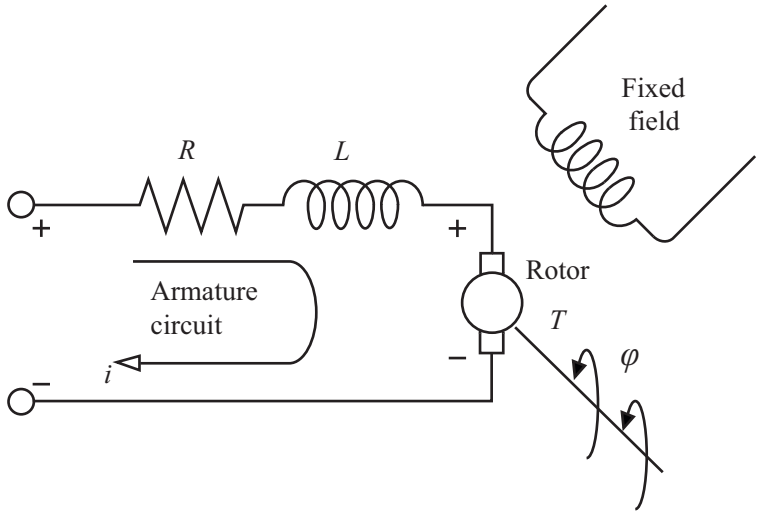


Figure 2: **Diagram of an electric motor (Adapted from Nise, 2007).**

The torque of the motor is proportional to the current that crosses the armature, thus arising Eq. (6).

$$T_m = K_t i \tag{6}$$

Where $K_t$ is a constant called constant of torque (Nise, 2007).
The back EMF (Electromotive Force) is proportional to the angular speed of the motor, and can be given by the Eq. (7).

$$V_b = K_b \dot{\varphi} \tag{7}$$

Where $V_b$ is a proportional constant. Now, using the Newton's Second Law, the dynamical equation of the DC motor can be deduced. This equation is shown in Eq. (8).

$$J\ddot{\varphi} + b\dot{\varphi} = K_t i \tag{8}$$

Where $b$ is the viscous friction of the motor mechanical parts.
The motor's electrical equation can be obtained with the help of the Kirchhoff's circuit laws as show in Eq. (9).

$$L\frac{di}{dt} + Ri = V - K_b\dot{\varphi} \tag{9}$$

Where $V$ is the voltage applied in the motor.
It is now possible to add the equations of the motor in the equations previously obtained from the non-ideal system. Equation (4) and Eq. (5) are rewritten as follows:

$$M\ddot{x} + c\dot{x} + kx - mr(\dot{\varphi}^2 sin\varphi + \ddot{\varphi}cos\varphi) = 0 \tag{10}$$

$$\left(J + mr^2\right)\ddot{\varphi} + mr\ddot{x}cos\varphi = K_t i - b\dot{\varphi} \tag{11}$$

$$\frac{di}{dt} = \frac{-K_b\dot{\varphi} - Ri}{L} \tag{12}$$

### 2.2 Numerical Simulations

For the numerical simulations, the Matlab® software was used. Before the numerical integration of the model shown in Eq. (10), Eq. (11) and Eq. (12), the system had to be reduced to first order differential equations. Making the following substitutions: $x_1 = x$, $x_2 = \dot{x}$, $\dot{x}_2 = \ddot{x}$, $x_3 = \varphi$, $x_4 = \dot{\varphi}$, $\dot{x}_4 = \ddot{\varphi}$, $x_5 = i$, $\dot{x}_5 = \frac{di}{dt}$ and $u = V$, it is possible to obtain the set of equations of the non-ideal system.

$$\dot{x}_1 = x_2 \tag{13}$$

$$\dot{x}_2 = -\frac{cx_2}{M} - \frac{kx_1}{M} + \frac{mr(x_4^2 sinx_3 + \dot{x}_4 cosx_3)}{M} \tag{14}$$

$$\dot{x}_3 = x_4 \tag{15}$$

$$\dot{x}_4 = \frac{K_t x_5}{J + mr^2} - \frac{b x_4}{J + mr^2} + \frac{mr\dot{x}_2 cos x_3}{J + mr^2} \tag{16}$$

$$\dot{x}_5 = \frac{u}{L} - \frac{K_b x_4}{L} - \frac{R x_5}{L} \tag{17}$$

The initial conditions used were: $x_1(0) = 0$, $x_2(0) = 0$, $x_3(0) = 0$, $x_4(0) = 0$ and $x_5(0) = 0$.
Table 1 shows the parameters used in numerical simulations, where all these parameters were obtained experimentally.

Table 1: **System parameters.**

| **Quantity** | **Symbol** | **Value** |
|---|---|---|
| Mass of the System (kg) | $M$ | 0.135 |
| Stiffness (N/m) | $k$ | 900 |
| Damping (Ns/m) | $c$ | 0.09 |
| Unbalanced Mass (kg) | $m$ | 0.05 |
| Motor Resistance ($\Omega$) | $R$ | 50 |
| Motor Inductance (H) | $L$ | 0.004 |
| Motor Torque Constant (Nm/A) | $K_t$ | 0.067 |
| Back EMF Constant (Vs/rad) | $K_b$ | 0.067 |
| Viscous Friction (Nms/rad) | $b$ | $2.8\text{x}10^{-6}$ |
| Inertia of the Motor (kgm$^2$) | $J$ | $0.9\text{x}10^{-6}$ |
| Eccentricity of the Shaft (m) | $r$ | 0.02 |

## 3. EXPERIMENTAL INVESTIGATION

### 3.1 Experimental Setup

For experimental results, a non-ideal system was constructed. The system consists of a cantilever aluminum beam with a DC motor attached to its free end. The motor is unbalanced by a small mass and, when the motor starts to work, the mechanical system begins to vibrate. Figure 3 shows the system described.

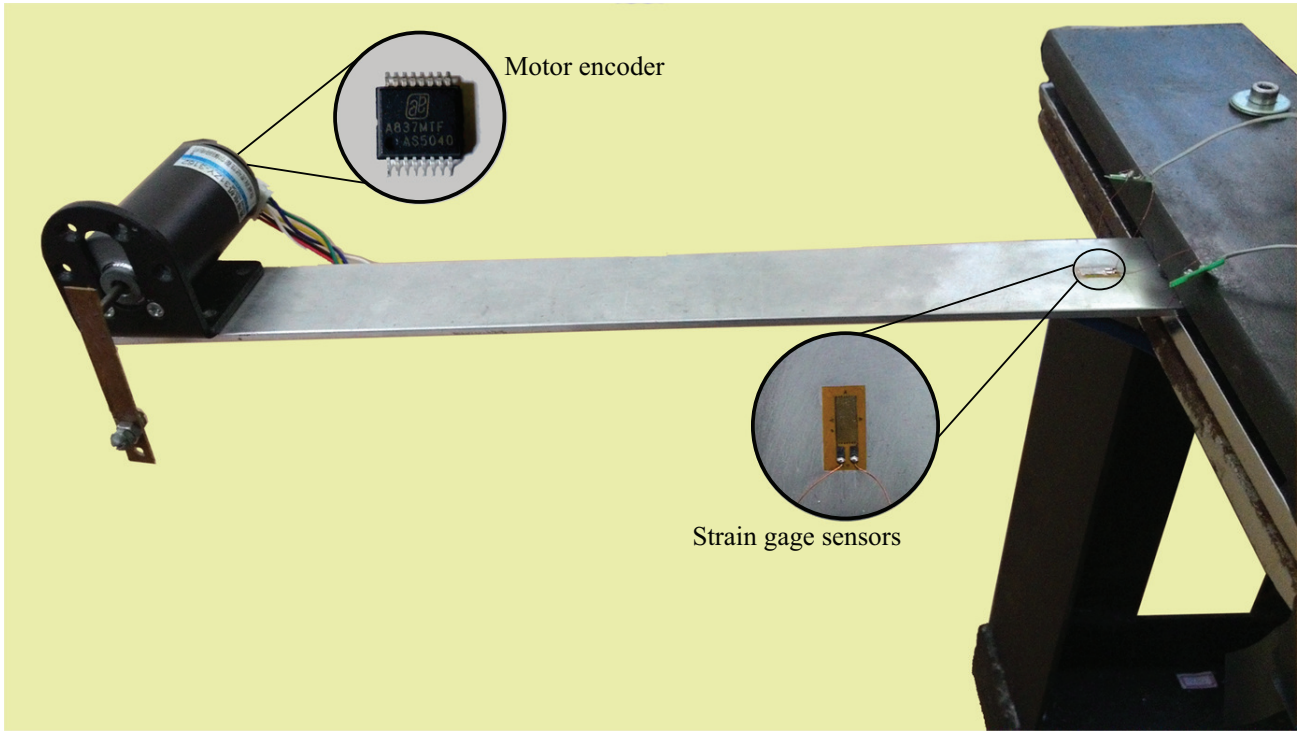


Figure 3: **Non-ideal system built.**

For the acquisition of system vibration, strain gage sensors were used. the signal was then amplified with the use of an amplification circuit made with an INA128 precision amplifier. All data were then captured with the aid of a DAq (Data Acquisition) model USB-6212. The instrumentation software used was the Labview®. Figure 4 shows a diagram of the data acquisition process used for the experimental results.

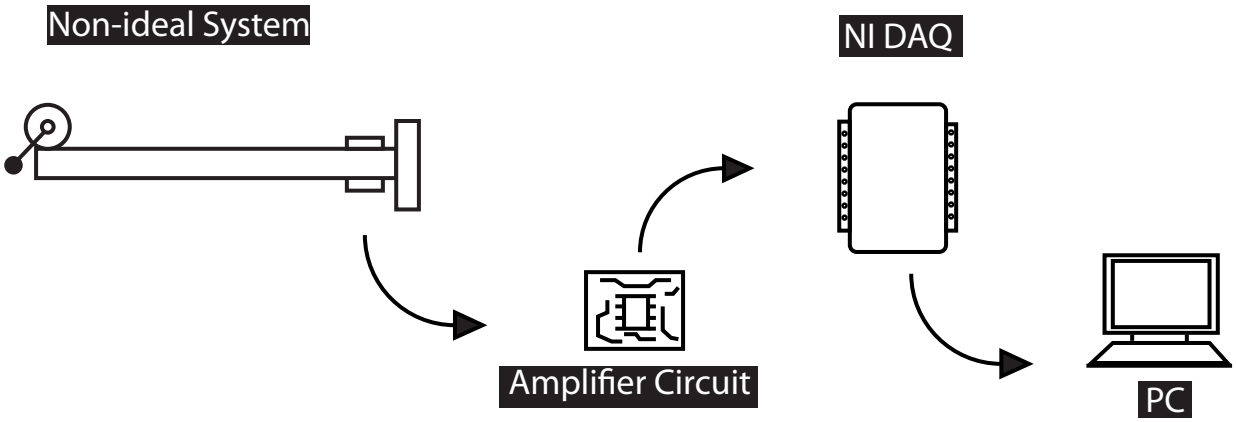


Figure 4: **Process of data acquisition.**

### 3.2 Experimental Procedure

For this paper, two types of Sommerfeld Effect graphs were obtained. The first graph is the jump effect considering the angular frequency of the motor. In this graph, the motor armature voltage was increased every 0.5 volts and the data of the vibration amplitude and angular frequency of the motor were saved. The second graph is the jump effect considering the voltage applied to the motor. This type of graph only considers the energy used in the system.

For the acquisition of data, the tests were executed more than once, where the best result was chosen.

## 4. RESULTS AND DISCUSSIONS

Figure 5 shows the graph of the jump effect as a function of the angular frequency of the motor. Numerical and experimental results are compared. As can be observed, the jump in the experimental result required a higher angular frequency to occur (82 rad/s and 116 rad/s respectively), but in contrast, the vibration amplitudes obtained the same value (about 0.033m).

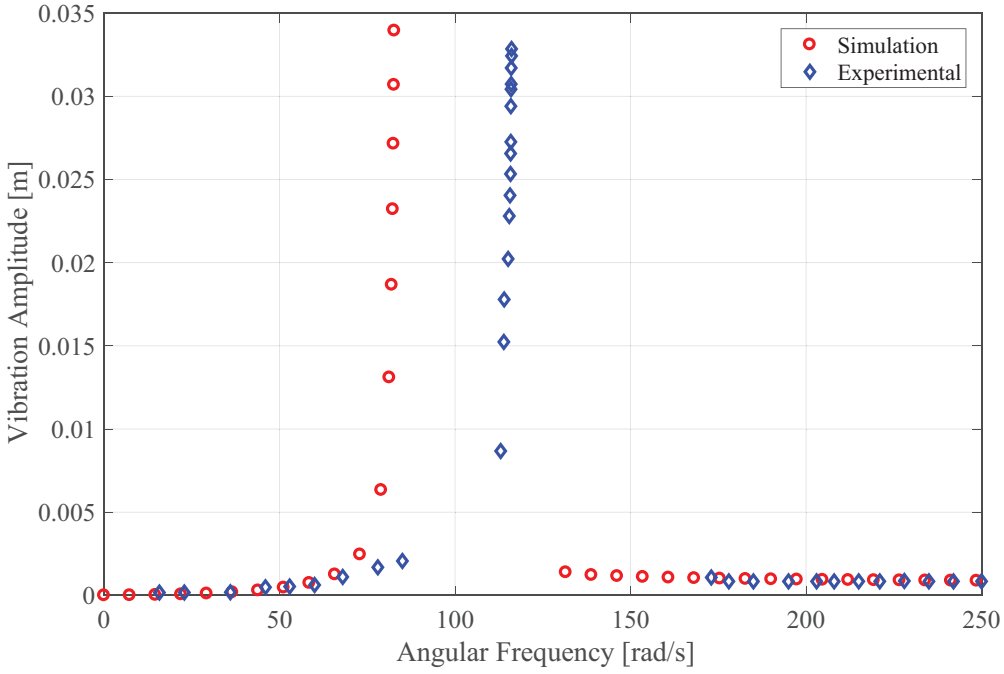


Figure 5: **Jump effect considering the angular frequency of the motor.**

Figure 6 shows the jump effect considering the voltage applied to the motor. With this type of graph, the direct influence of the energy used on the non-ideal system can be observed. Again, the experimental results had a little difference when compared to numerical results.The vibration amplitudes are the same as in Fig. 5, but there is a difference in the

occurrence voltage of the jump effect (8.5 V and 12.5 V, respectively). As can be observed by the results, the mathematical model obtained as well as the parameters used could be used to reproduce the Sommerfeld effect, the effects of the angular frequency curve discontinuity can easily be observed.

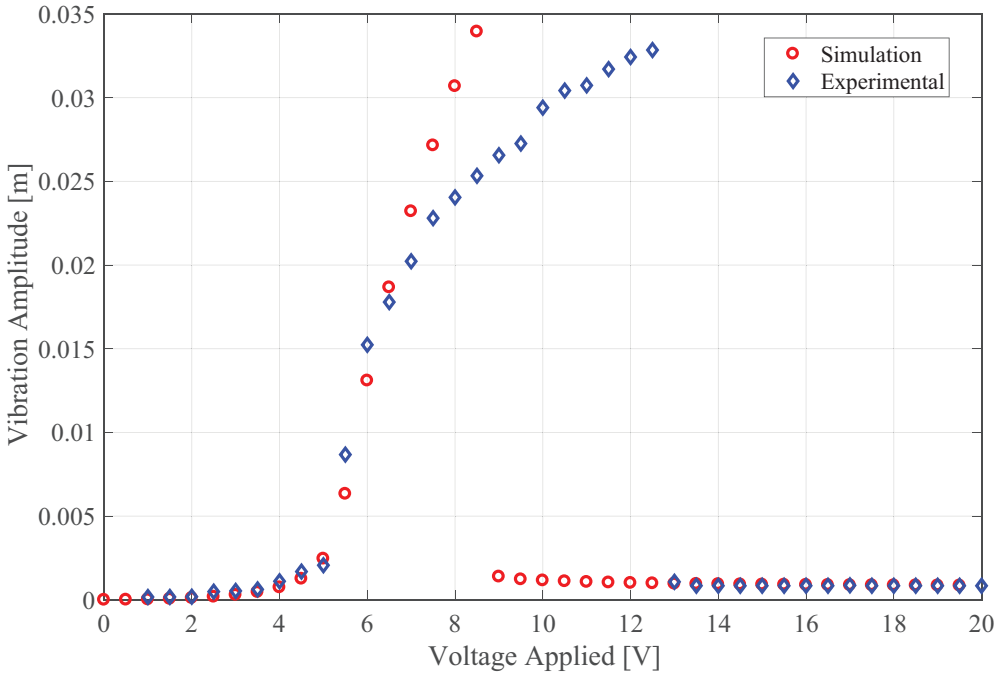


Figure 6: **Jump effect considering the electric voltage of the motor.**

Differences in experimental and numerical results may be caused by system parameters or by certain considerations in the model. Different energy losses can occur in the experimental system, in contrast to the numerical system, this can be one of the causes of the experiment system to need more energy to make the jump occur

## 5. CONCLUSIONS

Due to their greater complexity, the non-ideal systems still present as a challenge for mathematical design and understanding. In this type of system, the power supply is influenced by its own performance, experiencing a loss of energy when the system approaches the resonance region.

This work presented a comparison between analytical and experimental results for the Sommerfeld Effect (jump phenomenon) present in a non-ideal type system. This is the most common and characteristic effect of a non-ideal systems, characterized by a transformation of the energy used by the motor, previously used to control the speed, now transformed into mechanical vibration. The system chosen consists of a cantilever beam with an unbalanced electric DC motor at its free end. For the mathematical model, a system of lumped parameters was considered. The governing equations of this system were obtained with the use of Lagrange equations, considering the complete model of an electric DC motor. In the experimental stage, it has built a system equivalent to that used in the numerical stage. All the parameters used in the simulations were obtained using the experimental system

The results showed a good correlation between the mathematical model and the real system, showing that the chosen method to obtain the equations was able to capture the main characteristics of the non-ideal system. The differences between the results can be explained by some simplifications in the mathematical model and energy losses that can occur in the experimental system that were not considered.

## 6. ACKNOWLEDGMENTS

The authors thanks the CNPq (grant: 447539/2014-0), CAPES and FAPESP for financial support.

## 7. REFERENCES

Balthazar, J.M., Mook, D.T., Weber, H.I., Brasil, R.M., Fenili, A., Belato, D. and Felix, J.L.P., 2003. "An overview on non-ideal vibrations". *Meccanica*, Vol. 38(6), pp. 613–621.

Castão, K., Balthazar, J.M., Pontes, B.R. and Felix, J.L.P., 2008. "On the reduction of the sommerfeld effect in a non-ideal vibrating problem using a magneto-rheological damper". In *7th Brazilian Conference on Dynamics, Control and Applications-dincon*. pp. 7–9.

Felix, J.L.P., Balthazar, J.M. and Brasil, R.M., 2005. "On saturation control of a non-ideal vibrating portal frame foundation type shear-building". *Journal of Vibration and Control*, Vol. 11(1), pp. 121–136.

Kononenko, V.O., 1969. *Vibrating Systems with a Limited Power Supply*. Iliffe, 1st edition.

Kossoski, A., Tusset, A.M., Janzen, F.C., Rocha, R.T., Balthazar, J.M., Reyolando, M.L.E.F. and Nabarrete, A., 2018. "Jump attenuation in a non-ideal system using shape memory element". *MATEC Web of Conferences*, Vol. 148, p. 03003.

Nise, N.S., 2007. *Control Systems Engineering*. John Wiley & Sons.

## 8. AUTHORAL RESPONSIBILITY

The authors are solely responsible for the content of this work.